ADVANCED FUNCTIONAL MATERIALS

Supporting Information

for *Adv. Funct. Mater.*, DOI: 10.1002/adfm.201703982

Nanoformulation of Brain-Derived Neurotrophic Factor with Target Receptor-Triggered-Release in the Central Nervous System

*Yuhang Jiang, James M. Fay, Chi-Duen Poon, Natasha Vinod, Yuling Zhao, Kristin Bullock, Si Qin, Devika S Manickam, Xiang Yi, William A. Banks, and Alexander V. Kabanov**

Supplementary material

Nanoformulation of Brain Derived Neurotrophic Factor with Target Receptor Triggered Release in Central Nervous System

Yuhang Jiang[1,2,†], James M. Fay[2,3], Chi-Duen Poon[4], Natasha Vinod[2,5], Yuling Zhao[1,2], Kristin Bullock[6], Si Qin[1,2], Devika S. Manickam[1,2,‡], Xiang Yi[1,2], William A. Banks[6], and Alexander V. Kabanov[1,2,5,7,]*

[1] Division of Pharmacoengineering and Molecular Pharmaceutics, Eshelman School of Pharmacy, University of North Carolina, Chapel Hill, NC 27599-7362

[2] Center for Nanotechnology in Drug Delivery, Eshelman School of Pharmacy, University of North Carolina, Chapel Hill, NC 27599-7362

[3] Department of Biochemistry and Biophysics, School of Medicine, University of North Carolina, Chapel Hill, NC 27599-7260

[4] Research Computer Center, University of North Carolina, Chapel Hill, NC, 27599

[5] Joint UNC/NC State Department of Biomedical Engineering, University of North Carolina, Chapel Hill, NC 27599-7575

[6] Geriatric Research Education and Clinical Center, Veterans Affairs Puget Sound Health Care System, Seattle, WA and Division of Gerontology and Geriatric Medicine, Department of Medicine, University of Washington School of Medicine, Seattle, WA 98108

[7] Laboratory for Chemical Design of Bionanomaterials, Faculty of Chemistry, M.V. Lomonosov Moscow State University, Moscow, 117234, Russia

E-mail: kabanov@email.unc.edu; Phone: +1 (919) 537-3800; Fax: +1 (919) 962-9922

Corresponding Author

*Correspondence: Dr. Alexander V. Kabanov, Division of Pharmacoengineering and Molecular Pharmaceutics and Center for Nanotechnology in Drug Delivery, UNC Eshelman School of Pharmacy, University of North Carolina at Chapel Hill, Chapel Hill, NC 27599, USA.

Present Addresses

† Department of Biomedical Engineering, Yale University, New Haven, CT, 06511.

‡ Pharmaceutical Sciences Division, Graduate School of Pharmaceutical Sciences, Duquesne University, Pittsburgh, PA 15282.

Supplementary Methods

Chemicals

Methoxy-poly(ethylene glycol)-*block*-poly(L-glutamic acid sodium salt) (PEG-PLE) was purchased from Alamanda Polymers™ (Huntsville, AL). Its molecular mass determined by gel permeation chromatography was 13 KDa, and polydispersity index was 1.00-1.20; the PEG molecular mass was 4.5 - 5.5 KDa and the degree of polymerization of the PLE block was 45-55. Recombinant human BDNF was purchased from PeproTech (Rocky Hill, NJ). Human Serum Albumin (HSA), Bovine Serum Albumin (BSA) powder, and SuperSignal™ West Pico Chemiluminescent Substrate was from Thermo Fisher (Waltham, MA). Lactate buffered Ringer's solution (LR), uranyl acetate, Protease&phosphatase Inhibitor Cocktail, and agarose tablet were purchased from Fisher Scientific. Chloramine T, RIPA Buffer, urethane, 3,3´-diaminobenzidine, isopentane, and IgG from human serum were purchased from Sigma-Aldrich (St. Louis, MO); Mini-PROTEAN® TGX™ Precast Protein Gels, bio-safe Commassie stain solution, sample loading and running buffers for electrophoresis were purchased from Bio-rad (Hercules, CA). Recombinant human TrkB Fc chimera protein (TrkB-Fc) was purchased from R&D systems (Minneapolis, MN). $Na^{125}I$ was purchased from PerkinElmer Life Sciences (Boston, MA); GlutaMAX™ high glucose Dulbecco's Modified Eagle Medium (DMEM) was purchased from Invitrogen (Carlsbad, CA); Anti-Phospho-TrkA (Tyr490)/TrkB (Tyr516) rabbit monoclonal antibody (used in 1:1000 dilutions in 5% BSA), Anti-Phospho-p44/42 MAPK (ERK1/2) (Thr202/Tyr204) rabbit polyclonal antibody (used in 1:1000 dilutions in 5% BSA), Anti-p44/42 MAPK (ERK1/2) Rabbit monoclonal Antibody (used in 1:1000 dilutions in 5% non-fat dry milk), and HRP-conjugated secondary antibodies was purchased Cell Signaling Technologies (Beverly, MA); Anti-TrkB rabbit polyclonal antibody (used in 1:2000 dilutions in 5% non-fat dry milk) was purchased from Millipore (Bedford, MA); Tris-buffered saline (TBS) and Tris-buffered saline with 0.1% Tween 20 (TBST) 10X stock solutions were purchased from Boston Bioproducts (Ashland, MA).

Isothermal titration calorimetry (ITC)

ITC measurements were performed at 25.0 °C by using an auto-ITC200 titration calorimeter (Malvern Instruments, MA). The sample cell was loaded with 360 µl of BDNF solution (12.5 µM) in 10mM phosphate buffer, pH 7.4 and titrated with 1 mM PEG-PLE solution in 2 µL aliquots with 3 minute intervals. The first injection was 0.2 µL. We used MicroCAl ORIGIN software to determine the site binding model, which provided the best fit (lowest $\chi 2$ value) in order to obtain ΔH^0, K_d, and the stoichiometry of association. ΔG^0 and ΔS^0 were obtained using the following equations.

$$\Delta G = \Delta H - T\Delta S$$

$$\Delta G = \mathrm{RT}\ln k$$

Molecular dynamic (MD) simulation

MD simulations were performed in GROMACS 4.6.3 using OPLS-AA force field with slightly modified parameters to suit for PEG-PLE simulation as previously reported for PEGylated proteins[1]. We extracted the monomer structure (PDB ID 1BND) and constructed a dimer by placing to copies in close vicinity and performing a molecular dynamics simulation until steady state was achieved. We generated a simulation

box around the protein and polymers using the *editconf* module of the *GROMACS* package. The dimensions were selected so that the minimum distance between the protein molecule and the edge of the box was 9 Å. Protein models were solvated with the TIP4P water model and, wherever necessary, the system was neutralized with Na^+ and Cl^- ions using the program genbox. All MD simulations were performed at constant temperature of 300K and pressure of 1bar for a time period of 100 ns. The electrostatic surface potential of BDNF dimer was calculated using APBS tool 2.1. The numbers of hydrogen bonds and non-bonding contacts in the trajectory were calculated using HBplus program at each step of the trajectory [2] with parameters set the same as described by Baker and Hubbard[3] for maximum comparability. The amino acid sequences forming the β-sheets and β-turns on BDNF were identified by PDBsum: https://www.ebi.ac.uk/thornton-srv/databases/cgi-bin/pdbsum/GetPage.pl?pdbcode=1bnd.

Protein thermal shift (PTS) assay

Samples were prepared by mixing 2 μg of BDNF or equivalent amount of Nano-BDNF ($Z_{-/+}$ = 1, 5, and 10) with the environmentally sensitive dye provided in the Protein Thermal Shift™ Dye Kit (Thermo Fisher). We performed the PTS assay using an Applied Biosystems® StepOnePlus™ 7500 Real-Time PCR system, and increased the temperature at a rate of 0.395°C/min. Melting temperature (T_m) was visualized by plotting the negative first-order derivative of fluorescence over temperature (-dF/dT) versus temperature (T), and determined as the local minimum of the curve in the range of 70°C to 95°C.

Statistical analysis

Statistical analysis was done using Prism 6.01 software (GraphPad, CA). Statistical differences between treatment groups were determined using unpaired Student's t-test for groups of two and one-way ANOVA followed by Tukey's multiple comparison test for groups of three and above. A P-value less than 0.05 was considered significant. Results of all experiments are presented as mean ± SEM unless otherwise specified.

Figures and Tables

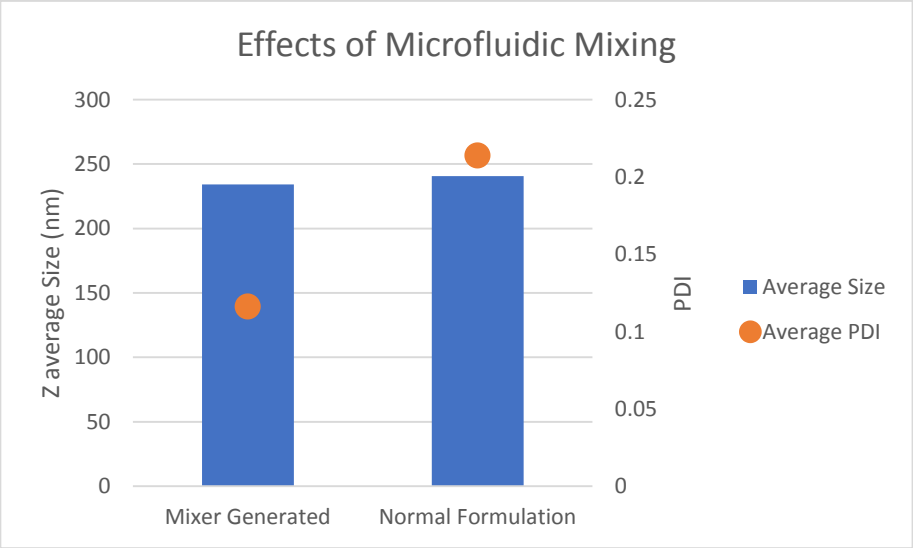

Figure S1. Microfluidic rapid mixing lowers the PDI of Nano-BDNF at $Z_{-/+}$ of 10.

Nano-BDNF was prepared using a microfluidic mixer (see **Figure S2**) and through manual mixing using a pipet and vortex. While sizes of the mixer-generated and manually prepared nanoparticles are similar (234 nm and 241 nm respectively) the PDI of the mixer-generated nanoparticle is 0.12 whereas the PDI of the ordinarily formulated Nano-BDNF is 0.21.

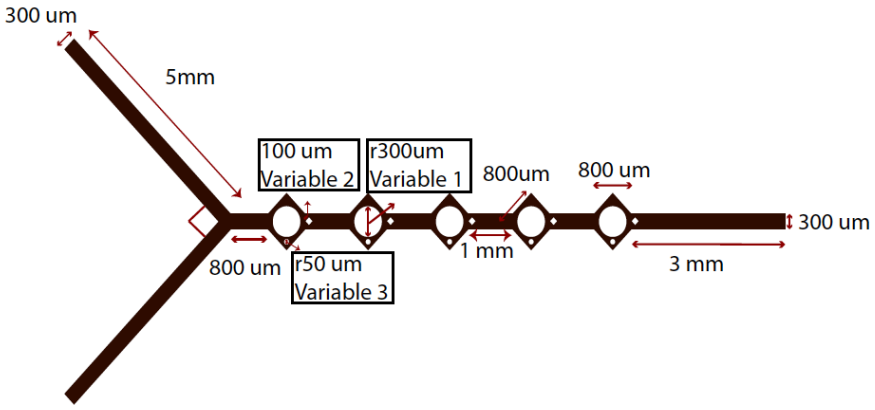

Figure S2. The schematic of the custom-made microfluidic mixer.

We used COMSOL multi-physics finite element modeling software to design a microfluidic mixer, which uses lamination[1] to achieve lateral mixing. The design model utilizes incompressible flow with convection and diffusion. Water density was set to 1 g/mL. We simulated mixing of a FITC dye with diffusivity of $0.5*10^{-9}$ m^2/s with water to determine mixing efficiency. The master device was fabricated using soft photolithography of a silicon wafer with Epoxy SU-8 photoresist. The final device was cast using PDMS (polydimethylsiloxane). We tested the device using FITC at 10 mM mixed with pure DI water at a flow rate of 10 μL/min. The mixer has a mixing efficiency of approximately 48.61 % at a Reynolds number of 1, which corresponds to a flow rate of 10 μL/min.

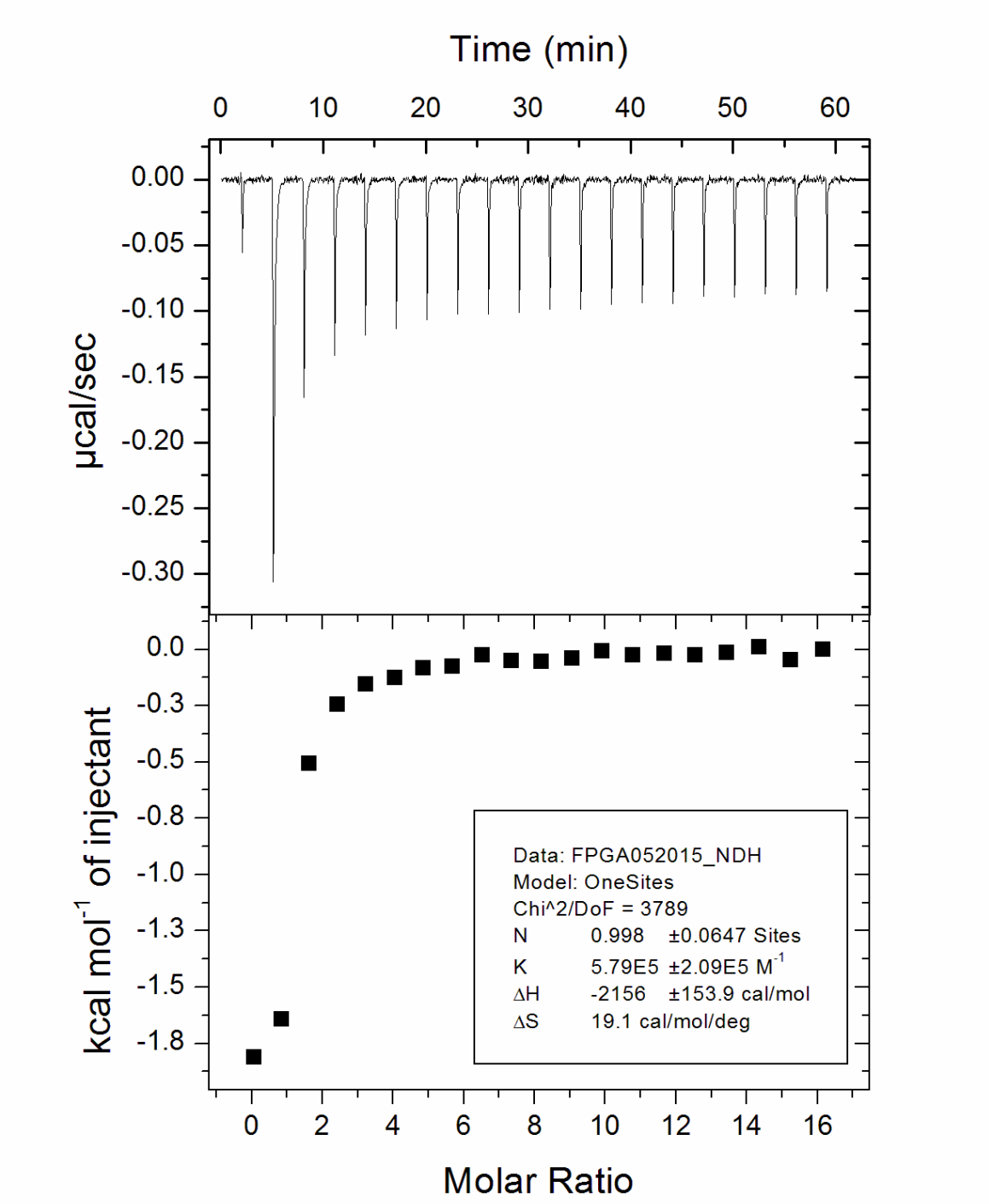

Figure S3. ITC measurement of complexation process between BDNF and PEG-PLE.

Both PEG-PLE and BDNF were dissolved in 10mM phostphate buffer, pH = 7.4. ITC data was obtained by slowly titrating PEG-PLE solutions into an isothermal chamber containing BDNF corroborates the saturation Z-/+ of Nano-BDNF to be between 6 and 7. The apparent K_d between mBDNF and PEG-PLE is around 1.8μM, assuming a one-site binding model which is consistent with the BDNF/TrkB binding mode.

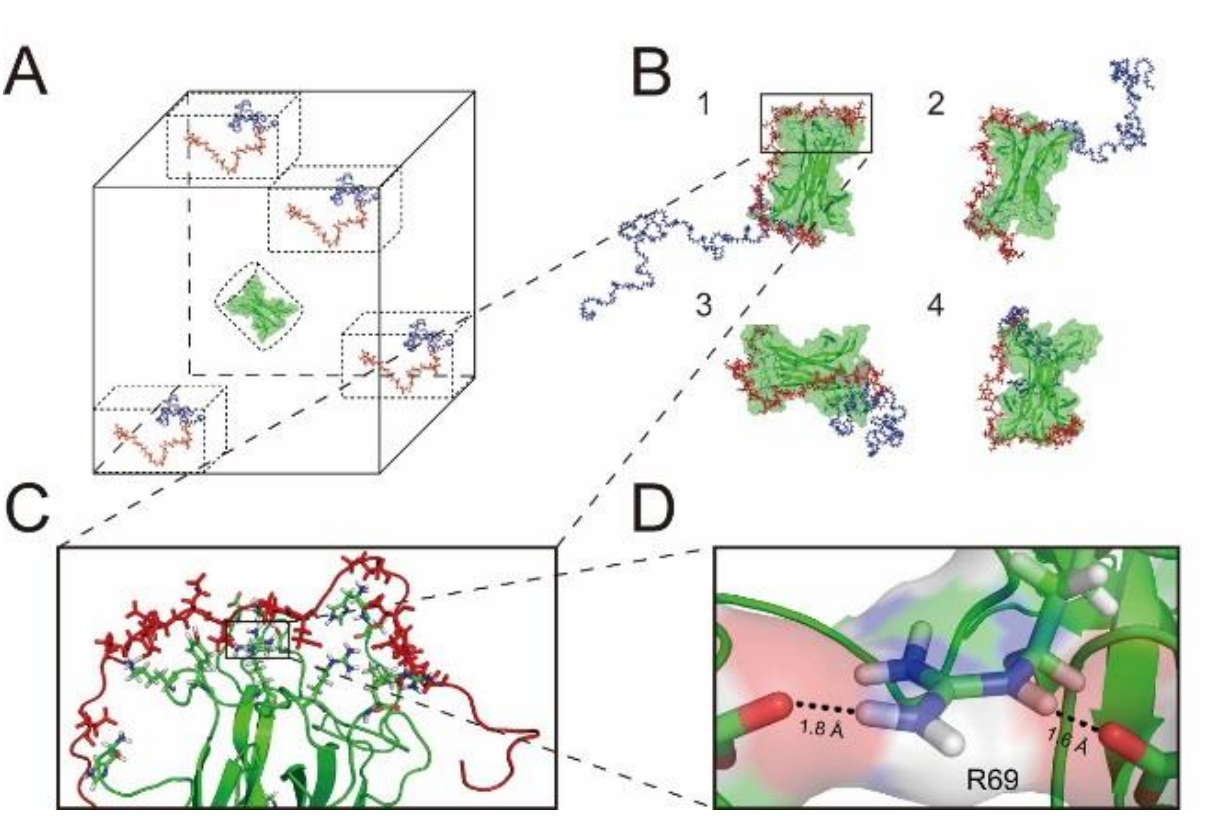

Figure S4. Molecular dynamics simulation.

A. Simulations were prepared with PEG-PLE in various starting positions (Boxed Polymers). **B.** Final frames of all the trajectories indicated tight binding between BDNF (visualized in cartoon mode) and PEG-PLE (visualized in stick mode) resulted from the simulations. **C.** Magnified picture of the squared area shown in **B**. The amino acids on BDNF that are within 3.9 Å of a glutamic acid residue on PEG-PLE are visualized in stick mode. **D.** Magnified picture of the squared area shown in **C**. Two hydrogen atoms on Arginine 69 of BDNF are shown to be located within 2 Å of oxygen atoms on PEG-PLE.

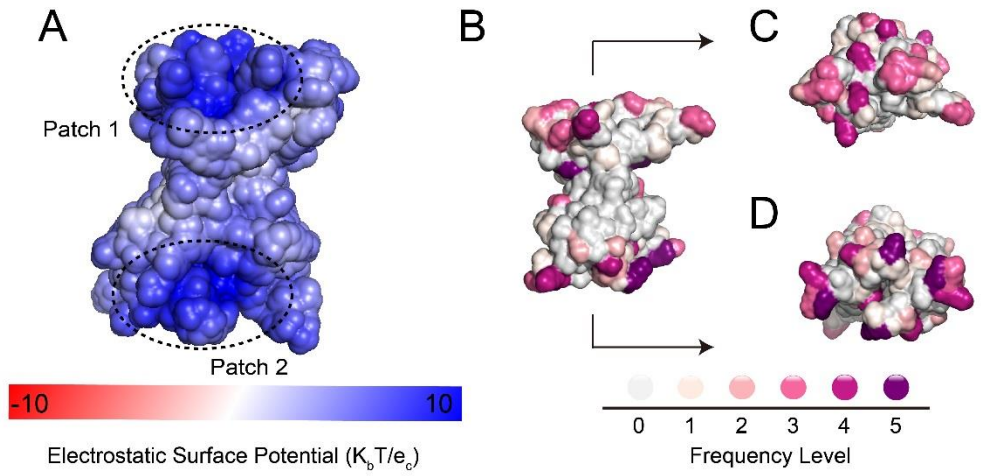

Figure S5. Identification of charge patches on BDNF and 3D density map of BDNF binding sites with PEG-PLE.

A. Electrostatic potential of BDNF plotted on the solvent-accessible surface. Potential surfaces are visualized ($-5K_bT/e_c$ (red) and $+5K_bT/e_c$ (blue) around a BDNF dimer molecule at pH 7.0, calculated with APBS tool 2.1. The two major cationic cavities are highlighted with the dashed circles. **B.** 3D-Heatmap of BDNF-polymer hydrogen bonds on each amino acid of BDNF. Frequency levels were defined in the same way as shown in Figure 3; **C.** Top view of **B.**; **D.** Bottom view of **B.** Frequency levels in **B**, **C**, and **D** are defined as described in Supplementary **Table S1**.

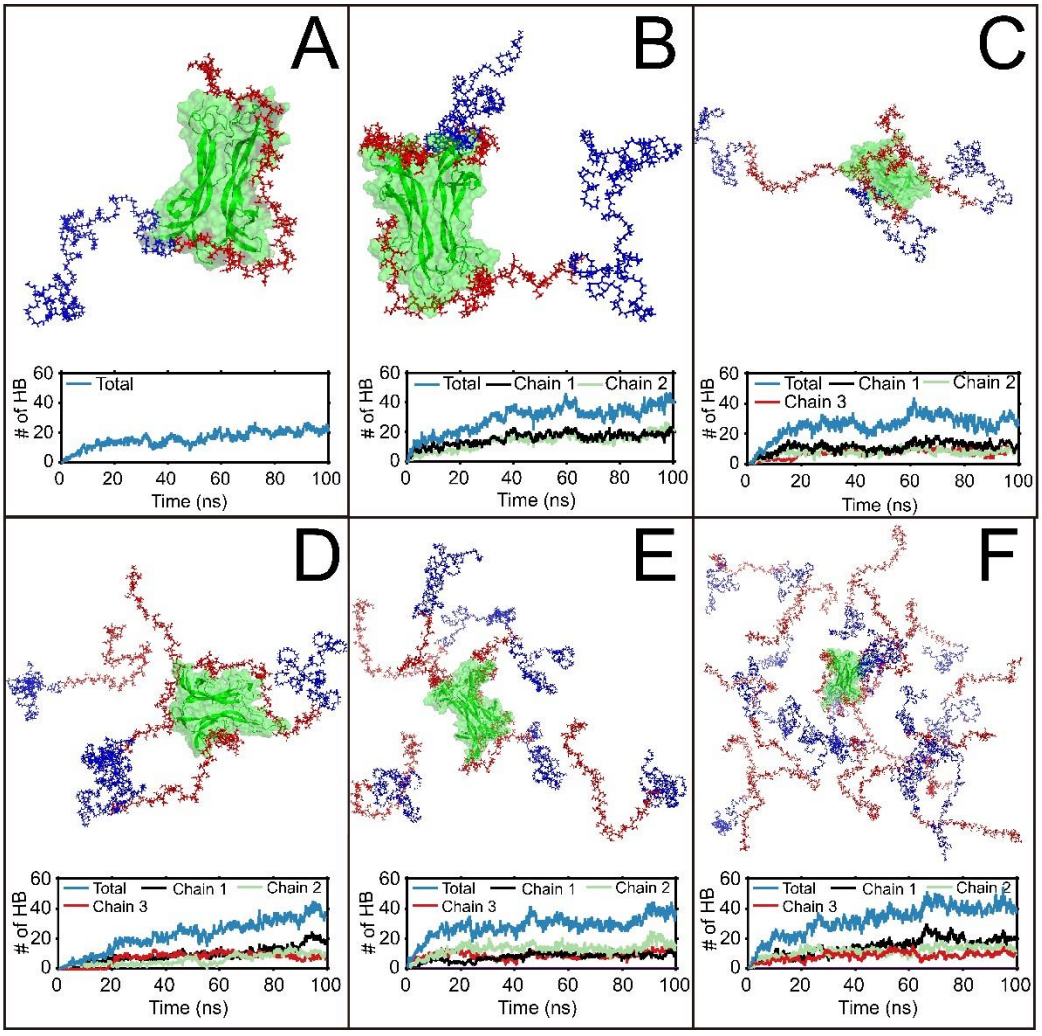

Figure S6. Molecular dynamics simulation of 1 BDNF molecule binding to different number of PEG-PLE chains.

A-F. Final frames of simulations with 1 BDNF molecule binding to 1, 2, 3, 4, 6, and 20 PEG-PLE chains, respectively. The number of hydrogen bonds occurred during the simulation were plotted against time: blue curves represent the total number of hydrogen bonds between BDNF and all polymer chains in the simulation; black, green, and red curves each represent the number of hydrogen bonds formed between BDNF and one single polymer chain. Green: cartoon and surface illustrations of a BDNF dimer molecule; Blue: stick illustration of PEG; Red: stick illustration of PLE. The number of hydrogen bonds formed was plotted as a function of simulation time under each graph. In all simulations, a maximum number of 3 polymer chains were observed to be able to form hydrogen bonds with the BDNF dimer.

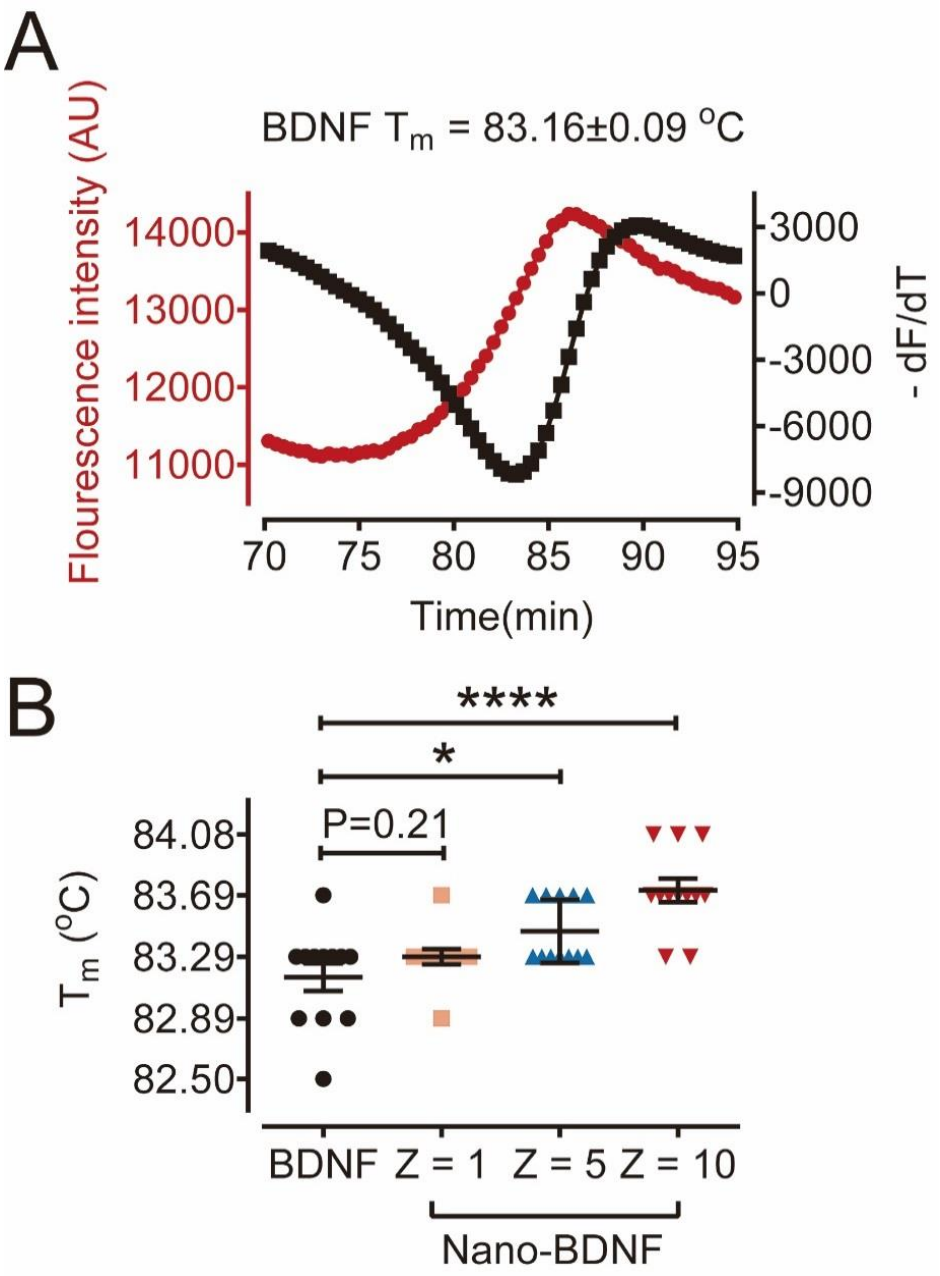

Figure S7. Protein thermal shift assay.

A. A representative graph demonstrating the melting curve of native BDNF in the proprietary assay buffer in the Protein Thermal Shift™ Dye Kit. The red dots denote fluorescent signal intensity (left Y-axis), and the black triangles denote the negative first-order derivative of fluorescent signal intensity (right Y-axis) in the temperature range of 70°C to 95°C. The T_m of native BDNF was determined to be 83.16 ± 0.09°C as described in the methods section. **B.** Scatter bar plot summarizing the T_m value of native BDNF and Nano-BDNF at $Z_{-/+}$ = 1, 5, and 10 (n = 12). Symbols above the horizontal lines denote significance levels compared to the native BDNF group, and are indicated by * ($P < 0.05$) and **** ($P < 0.0001$). This experiment was performed in 10mM phosphate buffer, pH = 7.4.

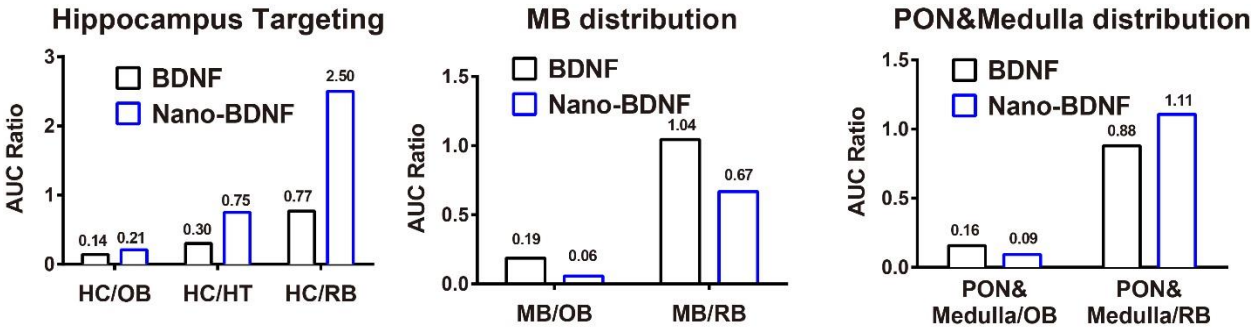

Figure S8. Nano-BDNF distribution in different brain regions after INB delivery compared to native BDNF.

Data present AUC ratios for the hippocampus (HC), pons (PON) and medulla, and midbrain (MB) vs. olfactory bulb (OB), hypothalamus (HT), and "rest of the brain" (RB) defined as all brain regions excluding HC and brainstem.

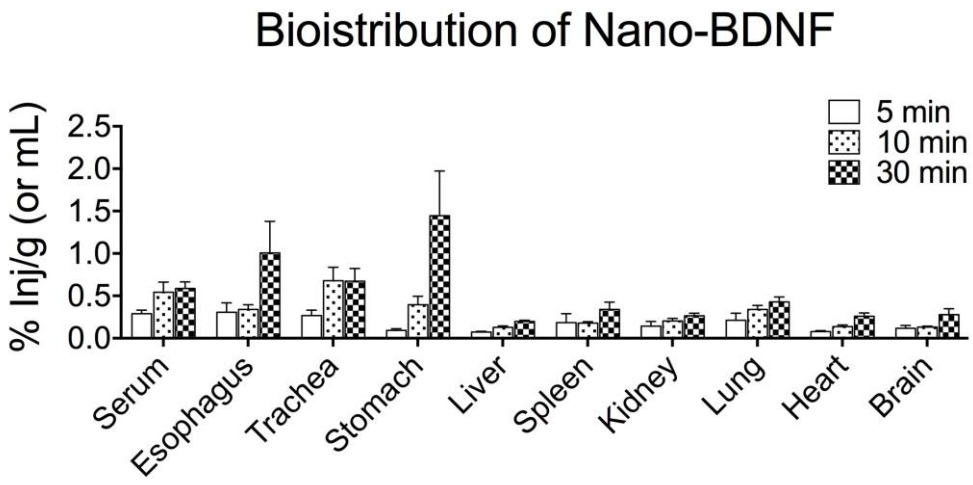

Figure S9. Biodistribution of Nano-BDNF following INB delivery.

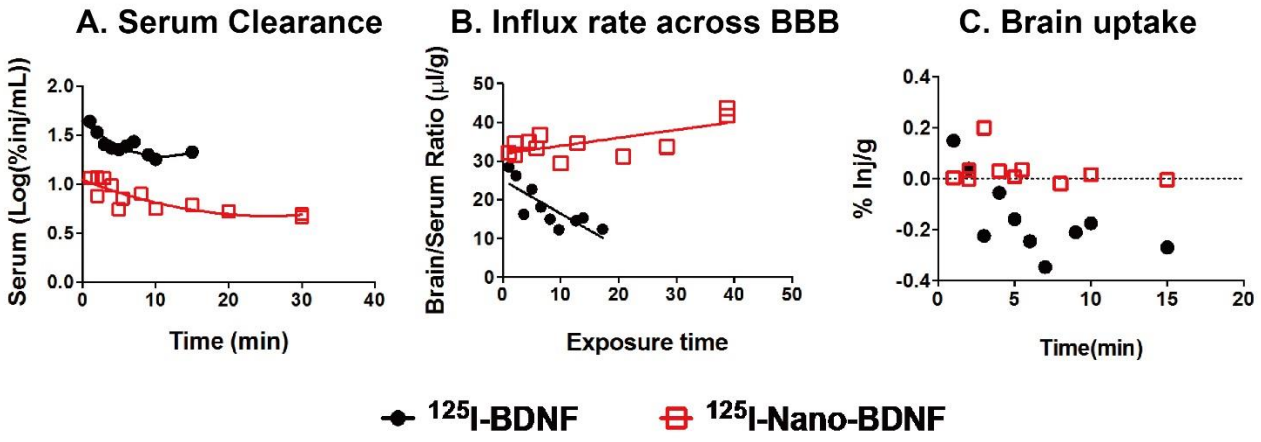

Figure S10. Brain PK of IV Nano-BDNF.

A. Nano-BDNF clears from the circulation similarly to native BDNF; **B.** Nano-BDNF displays net influx (Ki = 0.84 uL/g.min) into the brain, whereas native BDNF displays a net efflux from brain to the blood; **C.** Nano-BDNF displays higher brain uptake than native BDNF, as shown by AUC of 2.96 for Nano-BDNF vs 0.54 for native BDNF. The native BDNF or Nano-BDNF were injected IV at a single dose of 0.5 µg/mouse.

Table S1. Reference chart for the frequency levels shown in Figure 2 and Figure S5

Frequency level	Count_NC[a)]	Count_HB[b)]
0	0 - 100	0 - 100
1	100 - 1000	100 - 1000
2	1000 - 5000	1000 - 2000
3	5000 - 10000	2000 - 3000
4	10000 - 20000	3000 - 4000
5	> 20000	> 4000

[a)] Count_NC denotes the total number of non-bonding contacts.

[b)] Count_HB denotes the total number of hydrogen bonds formed across the entire process of the four simulation experiments.

Table S2. Summary of BDNF AUC values (%inj·min/g) in different brain regions

Region	BDNF	Nano-BDNF	Ratio
Olfactory	5.094	34.32	6.7
Striatum	1.860	4.923	2.6
Frontal Cortex	0.8850	2.033	2.3
Hypothalamus	2.145	9.588	4.5
Hippocampus	0.7300	7.229	9.9
Thalamus	0.6150	4.419	7.2
Parietal Cortex	0.6200	2.261	3.6
Occipital Cortex	0.9400	2.593	2.8
Cerebellum	0.9200	1.704	1.9
Midbrain	0.9500	1.929	2.0
Pons	0.7917	3.220	4.1
Whole Brain[a)]	1.020	3.550	3.5
Brainstem[b)]	0.7289	2.905	4.0
Serum	4.835	3.088	0.6

[a)] Whole brain AUC was calculated as the weight-averaged AUC of all the brain regions listed above (except brainstem).

[b)] Brainstem AUC was calculated as the weight-averaged AUC of midbrain and pons regions.

References

1. Mu, Q.; Hu, T.; Yu, J. Molecular insight into the steric shielding effect of PEG on the conjugated staphylokinase: biochemical characterization and molecular dynamics simulation. *PLoS One* 2013, 8, e68559.

2. McDonald, I. K.; Thornton, J. M. Satisfying hydrogen bonding potential in proteins. Journal of molecular biology 1994, 238, 777-93.

3. Baker, E. N.; Hubbard, R. E. Hydrogen bonding in globular proteins. Progress in biophysics and molecular biology 1984, 44, 97-179.